The CRS Method for Weakly Anisotropic VTI Media

Rodrigo Bloot * (CEPETRO/UNILA), Tiago A. Coimbra (CEPETRO/UNICAMP), Jorge H. Faccipieri(CEPETRO/UNICAMP) and Martin Tygel (IMECC/UNICAMP).

This paper was prepared for presentation at the 15[th] International Congress of the Brazilian Geophysical Society, held in Rio de Janeiro, Brazil, 31 July to 3 August, 2017.

Abstract

We describe an extension of the Common-Reflection-Surface (CRS) method for vertical tranversely isotropic (VTI) anisotropic media. The obtained second-order coefficients of the extended CRS traveltime explicitly depend on the Thomsen parameters that describe the VTI medium. Considering only the offset direction, the proposed CRS traveltime assumes a nonhyperbolic traveltime character which can be compared with VTI nonhyperbolic traveltimes that considers short-spread normal moveout velocities for plane horizontal reflectors. Numerical experiments showed that the proposed approach yields better traveltime approximations when an estimated stacking velocity is considered instead of short-spread normal moveout velocity.

Introduction

Since the pioneering work of Mann (1962), traveltime expressions designed for stacking along events of interest have always been a topic of active research in seismic reflection. Generally referred to as moveouts, these traveltimes originally aimed at non-converted primary reflections in isotropic media under the restrictions of common-midpoint (CMP) configuration and small offsets (see, e.g., Tygel and Santos, 2007; Iversen, 2006). Under these considerations, the first moveout, still routinely applied in today's seismic processing, is the normal moveout (NMO)(Taner and Koehler, 1969; Neidell and Taner, 1971). NMO is the simplest example of a hyperbolic (second-order Taylor polynomial of squared traveltime) traveltime.

In the 1980s, technological advances in seismic acquisition (e.g., larger offsets, ocean-bottom cables) posed the demand for a better understanding of wave propagation in anisotropic media, in particular weak elastic anisotropy (such as transversely isotropy (TI)) that are relevant for seismic processing (Helbig, 1983; Hake et al., 1984; Thomsen, 1986; Cohen, 1996; Alkhalifah, 2000; Grechka et al., 2004; Tsvankin, 2012; Bloot et al., 2013).

The description of anisotropy parameters given by Thomsen (1986) for TI media opened the analytic interpretation of anisotropy and allowed the development of moveouts for large offsets in terms of non-hyperbolic moveouts. Still within the the CMP configuration, a number of such anisotropic moveouts have been reported (Thomsen, 1993; Alkhalifah and Tsvankin, 1995; Tsvankin and Thomsen, 1994; Tsvankin, 1996; Fomel and Grechka, 2001).

By the end of 1990s, moveouts have been proposed free from the restriction of the CMP configuration. The two most prominent ones, all defined for isotropic media, are the Multifocus (MF) (Landa, 2007; Berkovitch et al., 2008; Landa et al., 2010) and the Common-Reflection-Surface (CRS) (Müller and Höcht, 1998; Perroud et al., 1999; Jäger et al., 2001; Hertweck et al., 2007; Fomel and Kazinnik, 2012) moveouts. The key motivation for those moveouts is to make full use of the multicoverage data (far greater than the CMP data), giving rise of much cleaner images. To achieve the extension to arbitrary configurations, the MF and CRS moveouts make use, besides the NMO velocity, of additional parameters. In 2D, the total number of parameters are three. In 3D, the CRS moveout depends on eight parameters. So far, there is no MF moveout available in 3D. The additional parameters have two impacts: The first and very positive one is that the new parameters provide useful kinematical information that can be applied to several purposes such as, e.g., migration (Coimbra et al., 2016), velocity building (Duveneck, 2004; Iversen and Tygel, 2008; Iversen et al., 2012; Gelius and Tygel, 2015), diffraction imaging (Dell and Gajewski, 2011; Faccipieri et al., 2016) and data regularization (Höcht et al., 2009). The second impact, which can be seen as a drawback, is that a greater number of parameters, as directly estimated by coherency analysis applied to the data leads to an increase of computer costs. The search of computer algorithms to retrieve CRS parameters in an efficient and reliable way is a topic of current investigation in the literature (Bonomi et al., 2014; Barros et al., 2015).

In this paper we describe an extension of CRS moveout for VTI anisotropic media. We show that the obtained moveout has the same form of the isotropic CRS moveout, in which the parameters are explicitly given by means of a multiplying factor that depends on the Thomsen parameters (Thomsen, 1986) that characterize the VTI media. Also, strategies to obtain information about anisotropy for large offsets will be discussed.

Formulation

We consider 2D seismic reflection data acquired along a single, horizontal line. On that line, source-receiver pairs are specified by midpoint and half-offset coordinates (m,h). We consider a super gather of source-receiver pairs arbitrarily located with respect to a reference or central zero-offset pair $(m_0,0)$. For a target (unknown) depth reflector and under the assumption of a vertical transversely isotropic (VTI) medium, our aim is to find an approximation of the reflection traveltime (moveout) on that super gather. For simplicity, we assume primary, non-converted reflections.

Isotropic medium: Our starting point is the conventional 2D CRS moveout in an isotropic medium, which is given by (Jäger et al., 2001)

$$t^2(m,h) = [t_0 + A\Delta m]^2 + B\Delta m^2 + Ch^2 \ , \quad (1)$$

Here, $\Delta m = m - m_0$ is the midpoint displacement relative to the central midpoint, m_0, and T_0 is the traveltime along the zero-offset ray (two-way traveltime along the normal ray) from the central point to the target reflector. As seen below, the parameters $A = A(m_0,T_0)$, $B = B(m_0,T_0)$ and $C = C(m_0,T_0)$ can be interpreted as kinematical attributes of the seismic propagation involved (see Equations 14-15. Moreover, reciprocity associated with symmetric reflections (see, e.g., Tygel and Santos, 2007) as in the case of primary non-converted reflections here considered, explains the absence (vanishing) of a linear coefficient in h.

Remark: Concerning the CRS moveout Equation 1, we make the following remarks:

(i) In the case of a CMP gather, defined by setting $m = m_0$ in Equation 1, the CRS traveltime reduces to the familiar normal moveout (NMO) traveltime, namely,

$$t^2_{CMP}(h) = t^2_{CRS}(m = m_0,h) = t_0^2 + Ch^2, \quad (2)$$

In particular, we see that

$$V^2_{NMO} = 4/C \ , \quad (3)$$

where V_{NMO} is the NMO-velocity at (m_0,T_0).

(ii) For a laterally invariant velocity distribution $V = V(z)$ and a planar horizontal reflector, the reflection traveltime is independent of midpoint m. As a consequence, the derivatives of traveltime with respect to m vanish. In this way, $A = B = 0$, leading to an identical moveout as the CMP expression 2.

VTI medium: Inspired by the nonhyperbolic moveout presented by Tsvankin and Thomsen (1994); Alkhalifah and Tsvankin (1995), which is valid for vertical transversely isotropic (VTI) media, we propose an extension of the CRS traveltime to those media in the form

$$t^2_a(m,h) = [t_0 + A_a\Delta m]^2 + B_a\Delta m^2 + C_a h^2 + f(h) \ , \quad (4)$$

where

$$f(h) = \frac{D_a h^4}{1 + (D_a/E_a)h^2} \ , \quad (5)$$

and

$$E_a = 4\left(\frac{1}{V_h^2} - \frac{1}{[V^{(a)}_{NMO}]^2}\right), \quad (6)$$

in which V_h is an effective horizontal velocity to be explained later and $V^{(a)}_{NMO}$ is defined as (compare with equation 3)

$$[V^{(a)}_{NMO}]^2 = 4/C_a. \quad (7)$$

Concerning the proposed weak anisotropy VTI moveout 4, the following considerations can be made:

1. For small offsets: $f(h) \approx D_a h^4$;

2. For large offsets: $f(h) \approx \left(\frac{4}{v_h(0)^2} - C_a\right)h^2$.

The first property indicates that the $f(h)$ acts as a fourth-order term of a Taylor expansion in offset direction. The second property means that, for a horizontal reflector within a constant VTI medium, the moveout Equation 4 is asymptotically exact in the offset direction as seen in Tsvankin and Thomsen (1994).

Remark: For the proposed VTI moveout Equation 4, the same observations made for the isotropic (CRS) moveout Equation 4 apply. Namely, both for the CMP configuration $(m = m_0)$ as for a planar horizontal reflector, the VTI moveout Equation 4 reduces to

$$t^2_a(m,h) = t_0^2 + C_a h^2 + \frac{D_a h^4}{1 + (D_a/E_a)h^2} \ . \quad (8)$$

We see, thus, that under the the circumstances of CMP configuration or a planar horizontal reflector, the proposed VTI moveout has the same form as the one proposed by Tsvankin and Thomsen (1994); Alkhalifah and Tsvankin (1995). As shown below, however, our proposed moveout has different expressions for the parameters.

Weak anisotropic VTI moveout

Transverse isotropic (TI) media, and as a consequence its particular case of vertical transversely isotropic (VTI) media, can be described in terms of Thomsen parameters (Thomsen, 1986). As shown in Bloot et al. (2013), the eikonal equation, which govern ray tracing in VTI media, has the form

$$V^2\left(\|\mathbf{p}\|^2 + 2\xi\|\widehat{\mathbf{p}}\|^2 + 2\zeta V_p^2 p_3^2\|\widehat{\mathbf{p}}\|^2\right) = 1 \ , \quad (9)$$

where V is the vertical velocity of the $q-P$, $q-SV$ or $q-SH$ waves. Moreover, ξ and ζ are corresponding wavemode quantities that depend on the Thomsen parameters ε, δ and γ. More specifically, we have

$$\text{q-P}: \quad V = V_p \ , \quad \xi = \varepsilon \ , \quad \zeta = \delta - \varepsilon \ , \quad (10)$$
$$\text{q-SV}: \quad V = V_s \ , \quad \xi = 0 \ , \quad \zeta = \varepsilon - \delta \ , \quad (11)$$
$$\text{q-SH}: \quad V = V_s \ , \quad \xi = \gamma \ , \quad \zeta = 0 \ . \quad (12)$$

As explained in (e.g., Červený, 2001), in an anisotropic media, the propagating direction of a ray is described by the group velocity vector. That vector points to the energy flux direction of the ray. In general, the group velocity vector differs in direction and amplitude from the phase velocity. The latter describes the propagation of wavefronts along the ray. Also relevant to the ray is the phase velocity vector which describes the propagation of the wavefront of the ray. The phase velocity vector is normal to the wavefront.

In the framework of weak anisotropic VTI medium, one can use paraxial ray approximations to find the following relations between the isotropic CRS parameters A, B and C and their counterpart anisotropic ones A_a, B_a and C_a given by

$$A_a = A = \frac{2\sin(\beta)}{V_0}, \quad (13)$$

$$B_a = H(\xi,\zeta)B = H(\xi,\zeta)\left[\frac{2t_0\cos^2(\beta)}{V_0}K_N\right], \quad (14)$$

$$C_a = H(\xi,\zeta)C = H(\xi,\zeta)\left[\frac{2t_0\cos^2(\beta)}{V_0}K_{NIP}\right]. \quad (15)$$

Here, β is the angle of the phase velocity (slowness vector) with respect to the vertical and V_0 is the phase velocity at the measurement surface. The quantities K_N and K_{NIP} represent the wavefront curvatures of the normal (N)-and normal-incidence-point (NIP)-waves measured at surface point $(m_0,0)$. Under the consideration of the point NIP where the reference normal ray hits the the target reflector, the N- and NIP-waves are two conceptual (fictitious) waves defined as follows: (a) The N-wave starts as a wavefront with the shape of the target reflector in the vicinity of NIP and (b) The NIP-wave starts as point source at NIP and progress to the surface. More details can be found, e.g., in Hubral (1983). Finally, $H(\xi,\zeta)$ denotes the anisotropy factor given by

$$H(\xi,\zeta) = \frac{1+\xi\sin^2(\beta)-\zeta\sin^2(\beta)\cos^2(\beta)}{1+2\xi\sin^2(\beta)+4\zeta(V_p/V_0)^2\sin^2(\beta)\cos^2(\beta)}. \quad (16)$$

In the case of $\xi=\zeta=0$, we have $H(\xi,\zeta)=1$. As a consequence, $A_a = A$, $B_a = B$ and $C_a = C$.

Remark: The quantities ξ, ζ, V_p and V_h refer to the reference point (m_0,t_0) upon which the Equation 4 is defined. As seen below, these quantities can be inverted from the parameters D_a and E_a.

Expression of parameters D_a and E_a

Under the condition that $K_N \approx 0$, the parameter D_a admits an explicit expression in terms of ξ and ζ. That assumption means that the obtained approximation is limited to small curvatures of shallow reflectors. As shown by Fomel and Grechka (2001), we have

$$D_a = \frac{4t_0(V_p/V_0)^2\zeta[1-L_1\tan(\beta)][\cos(\beta)+\sin(\beta)]K_{NIP}^3}{V_0L_2}, \quad (17)$$

where

$$L_1 = \frac{\sin(\beta)\left[1+2\xi+2\zeta(V_p/V_0)^2\cos^2(\beta)\right]}{L_2}, \quad (18)$$

in which

$$\begin{aligned} L_2 &= (1+2\xi)\sin(\beta)\tan(\beta)+\cos(\beta) \\ &+ 2\zeta(V_p/V_0)^2\cos^2(\beta)\sin(\beta)[\tan(\beta)+\sin(\beta)]. \end{aligned} \quad (19)$$

Finally, considering the heuristic assumption

$$V_h^2 \approx [V_{NMO}^2]^2 - \zeta V_p^2, \quad (20)$$

and substituting on Equation 6, we obtain

$$E_a = \frac{4}{[V_{NMO}^{(a)}]^2-\zeta V_p^2} - \frac{4}{[V_{NMO}^{(a)}]^2}. \quad (21)$$

Particular case: Horizontal plane wavefront emerging at the measurement surface

For comparison with the literature, it is interesting to investigate the situation when $\beta=0$, which includes the case of reflection of a plane reflector in a VTI medium. As previously indicated, we have in this case $H(\xi,\zeta)=1$. Setting $\beta=0$ in equations 15 and 17, we find

$$C_a = \frac{4}{[V_{NMO}^{(a)}]^2} = \frac{2t_0}{V_0}K_{NIP}, \quad (22)$$

and

$$D_a = 4t_0\zeta\frac{V_p^2}{V_0^3}K_{NIP}^3 = \frac{32\zeta V_p^2}{t_0^2[V_{NMO}^{(a)}]^6}. \quad (23)$$

Substitution of equations 22, 23 and 6 into equation 4 produces the proposed moveout t_a for the case $\beta=0$.

$$\begin{aligned} t_a^2 &= t_0^2 + \frac{4}{[V_{NMO}^{(a)}]^2}h^2 + \frac{32\zeta V_p^2}{t_0^2[V_{NMO}^{(a)}]^6}\times \\ &\times \left[1+\frac{8\left([V_{NMO}^{(a)}]^2-\zeta V_p^2\right)}{t_0^2[V_{NMO}^{(a)}]^4}h^2\right]^{-1} h^4. \end{aligned} \quad (24)$$

We now have the proper conditions to compare the proposed moveout (equation 24) with the one of (Alkhalifah and Tsvankin, 1995), here referred to as AT-moveout and denoted t_{AT}, for P-wave propagation, the latter being given by

$$t_{AT}^2 = t_0^2 + \frac{4}{[V_{NMO}^{(ss)}]^2}h^2 - \frac{32\eta h^4}{[V_{NMO}^{(ss)}]^2[t_0^2[V_{NMO}^{(ss)}]^2+4(1+2\eta)h^2]}. \quad (25)$$

Here, $V_{NMO}^{(ss)}$ and η are, respectively, the short-spread normal moveout velocity (Thomsen, 1986) and the anisotropy parameter

$$V_{NMO}^{(ss)} = V_p\sqrt{1+2\delta} \qquad \text{and} \qquad \eta = \frac{\varepsilon-\delta}{1+2\delta}. \quad (26)$$

Note that the velocities $V_{NMO}^{(a)}$ and $V_{NMO}^{(ss)}$ have very distinct expressions. The short-spread normal moveout, $V_{NMO}^{(ss)}$, was defined in Thomsen (1986) for a horizontal plane reflector and $V_{NMO}^{(a)}$ is related to the NIP-wave curvature K_{NIP}. In the homogeneous isotropic case both collapse to the same velocity. However, in the VTI media, the lateral velocity variation makes the NIP-wavefront change its format even in homogeneous case.

Analysis of moveout errors: It is now instructive to investigate the sensitivity of the non-hyperbolic terms in the above moveouts for a change in NMO velocities only. For that matter, we analyze the traveltime errors on three materials described on Table 1, whose experimental values are reported in Thomsen (1986). For each material, we consider a synthetic model with a single plane horizontal reflector, at 2 km depth, for which the seismic data were simulated by anisotropic ray tracing for 12 km maximum offset. Only P-waves were considered. Conventional velocity analysis, using a hyperbolic traveltime, was performed on the modeled CMP gather and the stacking velocity, V_{STK}, was estimated using the heuristic algorithm Differential Evolution (Barros et al., 2015) considering all traces.

The theoretical values of $V_{NMO}^{(a)}$ were computed from the second-derivative (parameter C_a) of the exact reflected traveltime for each material. Also, the values for $V_{NMO}^{(ss)}$ were computed by equation 26 upon considering the given values in Table 1.

Table 1: Anisotropic materials considered in the numerical experiments.

Material	v (m/s)	ε	δ
Taylor sandstone	3368	0.110	-0.035
Dry Green River Shale	3292	0.195	-0.220
Mesaverde sandstone	2998	0.010	0.012

For the case of Taylor sandstone, Figure 1 shows the relative error in offset direction of the proposed (black curve) and AT (red curve) moveouts with respect to the exact (modeled) moveout, both with their respective theoretical velocities and with the given modeled anisotropic parameters. The AT moveout outperforms the proposed moveout, achieving maximum relative error of 1% and good asymptotic approximation. The proposed traveltime presents less accuracy. In both cases, the maximum relative error does not exceed 2.5%, even considering an aperture of 12 km. However, when the estimated stacking velocity, V_{STK}, is considered, Figure 2 shows that the proposed moveout achieves better accuracy (less than 4%) than the AT moveout (less than 10%).

Its worth mentioning that the sensitivity of both moveouts differs when theoretical or estimated velocities are considered. Note that the proposed moveout shows smaller discrepancies between the theoretical and estimated velocities. The comparison of all velocities can be found in Table 2.

Table 2: Theoretical and estimated velocities obtained for each material.

Material	$V_{NMO}^{(ss)}$	$V_{NMO}^{(a)}$	V_{STK}
Taylor sandstone	3248	3377	3657
Dry Green River Shale	2463	2940	3715
Mesaverde sandstone	3033	3037	3029

Figure 3 shows the error considering the theoretical velocities with their respective traveltimes for Dry Green River Shale model. Again, the AT traveltime, using $V_{NMO}^{(ss)}$, showed a maximum relative error of 1% yielding a good asymptotic behavior on larger offsets. The proposed traveltime, using $V_{NMO}^{(a)}$, loses accuracy, presenting a maximum error of 5%. In the case of using the estimated velocity, V_{STK}, the pattern observed on the previous example is present, as shown in Figure 4. Now, the proposed approach achieved a maximum error of 10% and AT obtained a maximum error of 30%. Once more, the comparison of the obtained velocities can be found in Table 2.

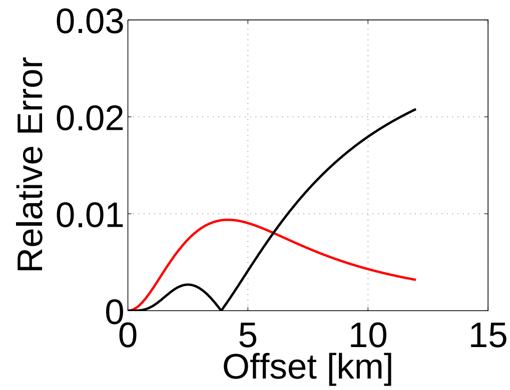

Figure 1: Taylor sand model: Relative error of the proposed (black solid line) and AT (red solid line) moveouts with respect to the exact (modeled) moveout. Theoretical velocities, $V_{NMO}^{(a)}$ and $V_{NMO}^{(ss)}$, respectively, have been taken.

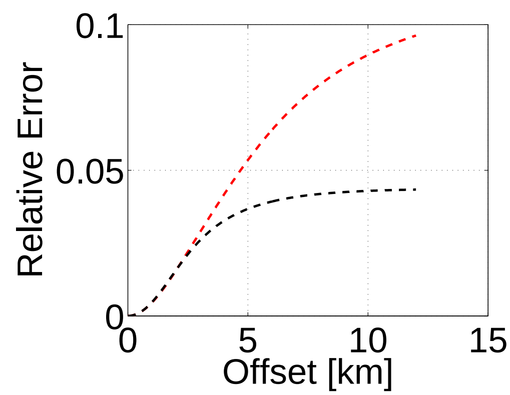

Figure 2: Taylor sand model: Relative error of the proposed (black dashed line) and AT (red dashed line) moveouts with respect to hyperbolic moveout with velocity, V_{STK}.

Elliptic anisotropy: When $\varepsilon = \delta$, which implies $\eta = \zeta = 0$, on Equations 24 and 25, both fourth-order terms vanishes and as a consequence, we have that $V_{NMO}^{(a)} = V_{NMO}^{(ss)}$. Despite the fact that this condition does not exists in practice, it is interesting due to its algebraic simplicity. This way, we can conclude that $V_{NMO}^{(a)}$ and $V_{NMO}^{(ss)}$ will be exactly the same only for isotropic media where we have $\zeta = \eta = 0$.

Even knowing that the elliptic case does not occur in reality it is interesting to observe the condition $\varepsilon \approx \delta$. Mesaverde immature sandstone described in Table 1 can be seen as a good example. In this case we have $V_{NMO}^{(a)} \approx V_{NMO}^{(ss)}$ so that the term D_a takes the form

$$D_a = 4t_0\zeta\frac{V_p^2}{V_0^3}K_{NIP}^3 \approx \frac{-32(\varepsilon-\delta)}{V_p^4(1+2\delta)^3t_0^2} = \frac{-32\eta}{T_0^2[V_{NMO}^{(ss)}]^4}. \quad (27)$$

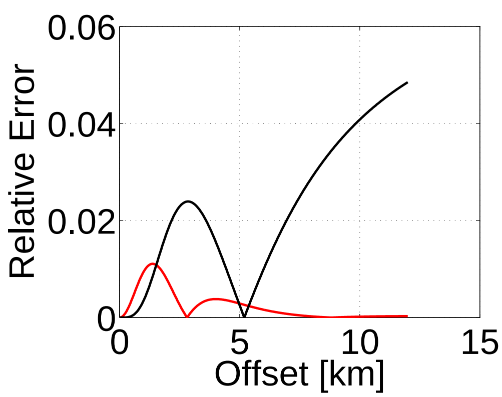

Figure 3: Dry Green River shale model: Relative error of the proposed (black solid line) and AT (red solid line) moveouts with respect to the exact (modeled) moveout. Theoretical velocities, $V_{NMO}^{(a)}$ and $V_{NMO}^{(ss)}$, respectively, have been taken.

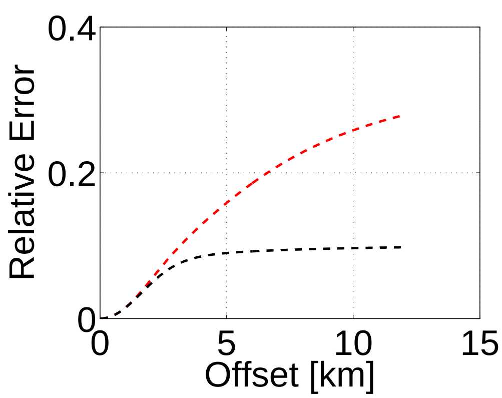

Figure 4: Dry Green River shale model: Relative error of the proposed (black dashed line) and AT (red dashed line) moveouts with respect to hyperbolic moveout with velocity, V_{STK}.

This means that the our approach coincides with the AT moveout in the case of small offsets. Figure 5 and 6, and also Table 2, shows numerical experiments that confirms this hypothesis. Moreover, in this cases, the stacking velocity, V_{STK}, does not differs from the theoretical velocities.

Discussion and Conclusions

In this work we proposed a CRS traveltime for weakly anisotropic VTI media. In the 2D situation considered here, the proposed moveout consists of the addition of two terms: the first one is a three-parameter CRS-type hyperbolic term which depends on midpoint and half-offset; the second one is a two-term non-hyperbolic term that depends on half-offset only. The new moveout has the same form of the well-established Alkalifah-Tsvankin moveout, however with a different definition of the parameters.

In order to compare the new moveout with the literature, we consider the particular case where the normal ray (around which the moveout is defined) emerges at the

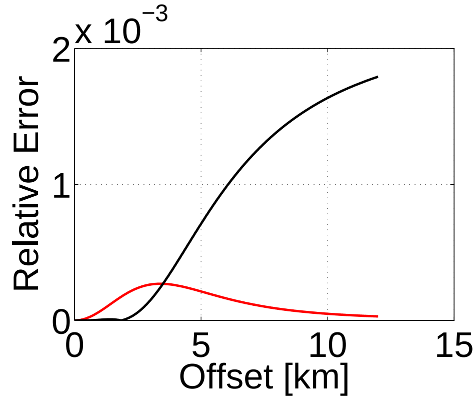

Figure 5: Mesaverde immature sandstone model: Relative error of the proposed (black solid line) and AT (red solid line) moveouts with respect to the exact (modeled) moveout. Theoretical velocities, $V_{NMO}^{(a)}$ and $V_{NMO}^{(ss)}$, respectively, have been taken.

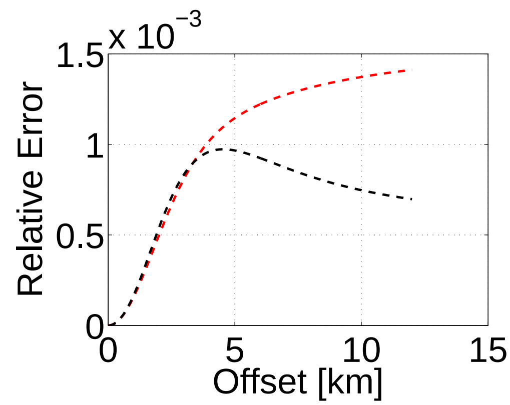

Figure 6: Mesaverde immature sandstone model: Relative error of the proposed (black dashed line) and AT (red dashed line) moveouts with respect to hyperbolic moveout with velocity, V_{STK}.

surface. This includes the case of a single plane horizontal reflector within a VTI medium and, in this way, it allows for a comparison with the well-established established Alkalifah-Tsvankin (TA) traveltime. Our numerical experiments considered two cases for the computation of the TA moveout: the first one used the exact short-spread normal moveout velocity of the model, the second one used the more practical situation of approximating that velocity by the stacking velocity estimated from the data. That estimation used the conventional velocity analysis with the hyperbolic moveout. Our results showed that the Alkalifah-Tsvanking moveout outperforms our proposed moveout when the exact short-spread normal moveout is taken. However, the use of the stacking velocity instead leads to better approximation of the proposed moveout. In addition, the results also suggest that the larger the difference between the Thomsen parameters ε and δ, the lower the accuracy is observed in the Alkalifah-Tsvankin moveout. Our analysis suggests that this happens because, in in this case, the short-spread normal moveout velocity differs more substantially from the estimated stacking velocity.

This conclusion is in accordance with the reported results in the literature.

Acknowledgments

We acknowledge support from the Center for Petroleum Studies (CEPETRO), the National Council for Scientific and Technological Development (CNPq-Brazil), the National Institute of Science and Technology of Petroleum Geophysics (ICTP-GP-Brazil) and the Center for Computational Engineering and Sciences (Fapesp/Cepid 2013/08293-7-Brazil). We also acknowledge support from the sponsors of the Wave Inversion Technology (WIT) Consortium and Petrobras.

References

Alkhalifah, T., 2000, An acoustic wave equation for anisotropic media: Geophysics, **65**, 1239–1250.

Alkhalifah, T., and L. Tsvankin, 1995, Velocity analysis for transversely isotropic media: Geophysics, **60**, 1550–1566.

Barros, T., R. Ferrari, R. Krummenauer, and R. Lopes, 2015, Differential evolution-based optmization procedure for automatic estimation of common-reflection surface traveltime parameters: Geophysics, **80**, WD189–WD200.

Berkovitch, A., I. Belfer, and E. Landa, 2008, Multifocusing as a method of improving subsurface imaging: The Leading Edge, **27**, 250–256.

Bloot, R., J. Schleicher, and L. T. Santos, 2013, On the elastic wave equation in weakly anisotropic VTI media: Geophysical Journal International, **192**, 1144–1155.

Bonomi, E., C. Tomas, P. Marchetti, and G. Caddeo, 2014, Velocity-independent and data-driven prestack time imaging: It is possible: The Leading Edge, **33**, 1008–1010.

Červený, V., 2001, Seismic ray theory: Cambridge University Press.

Cohen, J., 1996, Analytic study of the effective parameters for determination of the NMO velocity function in transversely isotropic media: Technical Report CWP, Colorado School of Mines, **CWP-191**.

Coimbra, T. A., D. S. R. J. H. Faccipieri, and M. Tygel, 2016, Common-reflection-point time migration: Studia Geophysica et Geodaetica, **60**, 500–530.

Dell, S., and D. Gajewski, 2011, Common-reflection-surface-based workflow for diffraction imaging: Geophysics, **76**, S187–S195.

Duveneck, E., 2004, 3d tomographic velocity model estimation with kinematic wavefield attributes: Geophysical Prospecting, **52**, 535–545.

Faccipieri, J. H., T. A. Coimbra, L.-J. Gelius, and M. Tygel, 2016, Stacking apertures and estimation strategies for reflection and diffraction enhancement: Geophysics, **81**, V271–V282.

Fomel, S., and V. Grechka, 2001, Nonhyperbolic reflection moveout of p-waves: An overview and comparison of reasons: CWP, **372**.

Fomel, S., and R. Kazinnik, 2012, Non-hyperbolic common reflection surface: Geophysical Prospecting, **61**, 21–27.

Gelius, L.-J., and M. Tygel, 2015, Migration-velocity building in time and depth from 3D (2D) Common-Reflection-Surface (CRS) stacking - theoretical framework: Studia Geophysica et Geodaetica, **59**, 253–282.

Grechka, V., L. Zhang, and J. W. Rector III, 2004, Shear waves in acoustic anisotropic media: Geophysics, **69**, 576–582.

Hake, H., K. Helbig, and C. Mesdag, 1984, Three term taylor series for t2-x2 curves of p and s waves over layered transversely isotropic ground: Geophysical Prospecting, **32**, 828–850.

Helbig, K., 1983, Elliptical anisoptropy—its significance and meaning: Geophysics, **48**, 825–832.

Hertweck, T., J. Schleicher, and J. Mann, 2007, Data stacking beyond CMP: The Leading Edge, **26**, 818–827.

Höcht, G., P. Ricarte, S. Bergler, and E. Landa, 2009, Operator-orientaded CRS interpolation: Geophysical Prospecting, **57**, 957–979.

Hubral, P., 1983, Computing true amplitude reflections in a lateeally inhomogeneous earth: Geophysics, **48**, 1051–1062.

Iversen, E., 2006, Tutorial: Amplitude, fresnel zone, and nmo velocity for pp and ss normal incidente reflections: Geophysics, **71**, W1–W14.

Iversen, E., and M. Tygel, 2008, Image-ray tracing for joint 3D seismic velocity estimation and time-to-depth conversion: Geophysics, **73**, S99–S114.

Iversen, E., M. Tygel, B. Ursin, and M. V. Hoop, 2012, Kinematic time migration and demigration of reflections in pre-stack seismic data: Geophysical Journal International, **189**, 1635–1666.

Jäger, R., J. Mann, G. Höcht, and P. Hubral, 2001, Common-reflection-surface stack: Image and attributes: Geophysics, **66**, 97–109.

Landa, E., 2007, Beyond conventional seismic imaging: EAGE.

Landa, E., S. Keydar, and T. J. Moser, 2010, Multifocusing revisited - inhomogeneous media and curved interfaces: Geophysical Prospecting, **58**, 925–938,.

Mann, H., 1962, Common relection point horizontal data stacking techniques: Geophysics, **27**, 927–938.

Müller, T., and G. Höcht, 1998, Common reflection surface staking method- imaging with an unknown velocity model: SEG Expanded Abstracts, **17**, 1764–1767.

Neidell, N., and M. Taner, 1971, Semblance and other coherency measures for multichannel data: Geophysics, **36**, 482–497.

Perroud, M., P. Hubral, and G. Höcht, 1999, Common-reflection-point stacking in laterally inhomogeneous media: Geophysical Prospecting, **47**, 1–24.

Taner, M. T., and F. Koehler, 1969, Velocity spectra-digital computer derivation and applications of velocity functions: Geophysics, **34**, 859–881.

Thomsen, L., 1986, Weak elastic anisotropy: Geophysics, **51**, 1954–1966.

——, 1993, Weak anisotropic reflections, *in* Offset dependent reflectivity: SEG, 103–114.

Tsvankin, I., 1996, P-wave signatures and notation for transverseley isotropic media: An overview: Geophysics, **61**, 467–483.

——, 2012, Seismic signatures and analysis of reflection data in anisotropic media: Pergamon Press.

Tsvankin, I., and L. Thomsen, 1994, Nonhyperbolic reflection moveout in anisotropic media: Geophysics, **59**, 1290–1304.

Tygel, M., and L. T. Santos, 2007, Quadratic normal moveout of symmetric reflections in elastic media: A quick tutorial: Studia Geophysics Geodetica, **2**, 533–540.